

Gold, iron and manganese in central Amapá, Brazil

Ouro, ferro e manganês na área central do Amapá, Brasil

Wilson Scarpelli^{1*}, Élio Hiromi Horikava²

ABSTRACT: Greenstone belts with deposits of gold, iron and manganese are common in the Paleoproterozoic Maroni-Itacaiunas Tectonic Province of the Guiana Shield. In Brazil, in the State of Amapá and northwest of Pará, they are represented by the Vila Nova Group, constituted by a basal unit of metabasalts, covered by metasediments of clastic and chemical origin. The basal metasediments, the Serra do Navio Formation, are made of a cyclothem with lenses of manganese marbles at the top of each cycle. Under the intense weathering of the Amazon, these lenses were oxidized to large deposits of high-grade manganese oxides. The exploitation of these oxides left behind the manganese carbonates and low-grade oxides. The overlying Serra da Canga Formation presents a calcium and magnesium domain grading to an iron domain with banded silicate and oxide iron formations, mined for iron ores. Overlapping structures and superposed metamorphic crystallizations indicate two phases of dynamothermal metamorphism, the first one with axis to north-northeast and the second one to northwest, with an intermediate phase of thermal metamorphism related to syntectonic granitic intrusions. Shears oriented north-south, possibly formed during the first dynamothermal metamorphism and reactivated in the second, are ideal sites for hydrothermalism and gold mineralization, which is greater when occurs in iron formation and carbonate-bearing rocks, as it happened at the Tucano mine. Layered mafic-ultramafic intrusions in the greenstones represent a potential for chromite and platinum group elements. Pegmatites are source of cassiterite and tantalite exploited from alluvial deposits.

KEYWORDS: Group Vila Nova greenstones; Manganíferous Precambrian cyclothem; Precambrian iron formation; Precambrian mafic-ultramafic complexes; Superposed metamorphic cycles.

RESUMO: A Província Tectônica Paleoproterozoica Maroni-Itacaiunas estende-se ao longo de toda a área costeira do Escudo das Guianas apresentando nessa extensão faixas de greenstone com depósitos hidrotermais de ouro. No Brasil, no estado do Amapá e no noroeste do Pará, os greenstones são representados pelo Grupo Vila Nova, que também apresenta depósitos sedimentares de ferro e de manganês e intrusões de complexos máfico-ultramáficos com possibilidades de mineralizações de cromo e platinoídes. Pegmatitos com cassiterita e tantalita são relacionados a intrusões graníticas sintectônicas nos greenstones. As faixas de greenstone Vila Nova cobrem embasamento de gnaisses, migmatitos e granitos. Em sua base há unidade de ortoanfibolitos, capeada por metassedimentos químicos e clásticos de granulação fina, na base dos quais há um ciclo tema com lentes de mármore manganífero no topo de cada ciclo. Na intemperização essas lentes foram substituídas por corpos massivos e de altos teores de óxido de manganês. As subsequentes unidades da coluna metassedimentar apresentam inicialmente domínio de cálcio e magnésio, gradando acima para um domínio de ferro, caracterizado por formações ferríferas silicáticas e oxidas, parte das quais são lavradas para minério de ferro. Corpos graníticos sintectônicos são intrusivos e formam domos no greenstone. Os greenstones foram submetidos a duas fases de metamorfismo dinamotermal, com uma fase intermediária de metamorfismo termal causada pelos granitos intrusivos. Zonas de cisalhamento formadas na primeira fase de metamorfismo e reativadas na segunda constituem locais favoráveis para a mineralização aurífera, principalmente quando em formações ferríferas.

PALAVRAS-CHAVE: Greenstones do Grupo Vila Nova; Ciclotema manganífero Precambriano; Formação ferrífera Precambriana; Complexos máfico-ultramáficos Precambrianos; Ciclos metamórficos superpostos.

¹Independent consultant. E-mail: wisicar@terra.com.br

²Independent consultant. E-mail: horikava@terra.com.br

*Corresponding author.

Manuscript ID 20170114. Received in: 08/25/2017. Approved in: 09/01/2017

INTRODUCTION

The objective of the authors is to divulge geological knowledge acquired throughout the years in exploration activities for deposits of iron, gold and manganese in the State of Amapá, Brazil, on behalf of Indústria e Comércio de Minérios S.A. (ICOMI), Unigeo Geologia e Mineração, Minorco Brasil, Anglo American do Brasil, AngloGold Ashanti, Min. Pedra Branca do Amapari, MMX Mineração, and others. It is expected that this note will help to understand the geology and mineral potential of the area and be useful in forthcoming mineral exploration there and elsewhere.

The described deposits occur in the Brazilian part of the Precambrian Guiana Shield (Fig. 1), which is constituted by four laterally collated tectonic provinces (Cordani & Teixeira 2007, Cordani *et al.* 2016), all of them containing Archean rocks metamorphosed into granitoids (gneisses, migmatites and intrusive granitic rocks), also presenting intrusive, volcanic, metamorphic and sedimentary units of variable ages.

At east, next to the coast, the Maroni-Itacaiunas (MI) Province is mostly made of Archean and Paleoproterozoic granitoids, also presenting belts of greenstone and associated intrusives, granulites, archean nuclei (Rosa-Costa *et al.* 2006), blocks of high metamorphic-grade rocks and granulites. The province was subject to several phases of tectonism and metamorphism, being tectonically stabilized at 2.26 to 2.01 Ga. From Venezuela to the Amazon Valley, the greenstones are remarkable for their mineral deposits of gold, iron and manganese, plus tantalum and tin in pegmatites. In Brazil, the province also contains stratiform deposits of chromite in intrusive layered mafic-ultramafic complexes (Spier & Ferreira Filho 2001).

Adjacent to the southwest, the Central Amazonian Province, stabilized at 2.03 to 1.88 Ga., contains several nuclei of Archean ages surrounded by Paleoproterozoic rocks and in the Middle Proterozoic received a large load of acid intrusives and extrusives in the south and of clastic sediments in the north. Next to west, the Ventuari-Tapajós Province, stabilized at 1.9 to 1.8 Ga., is composed by stacked

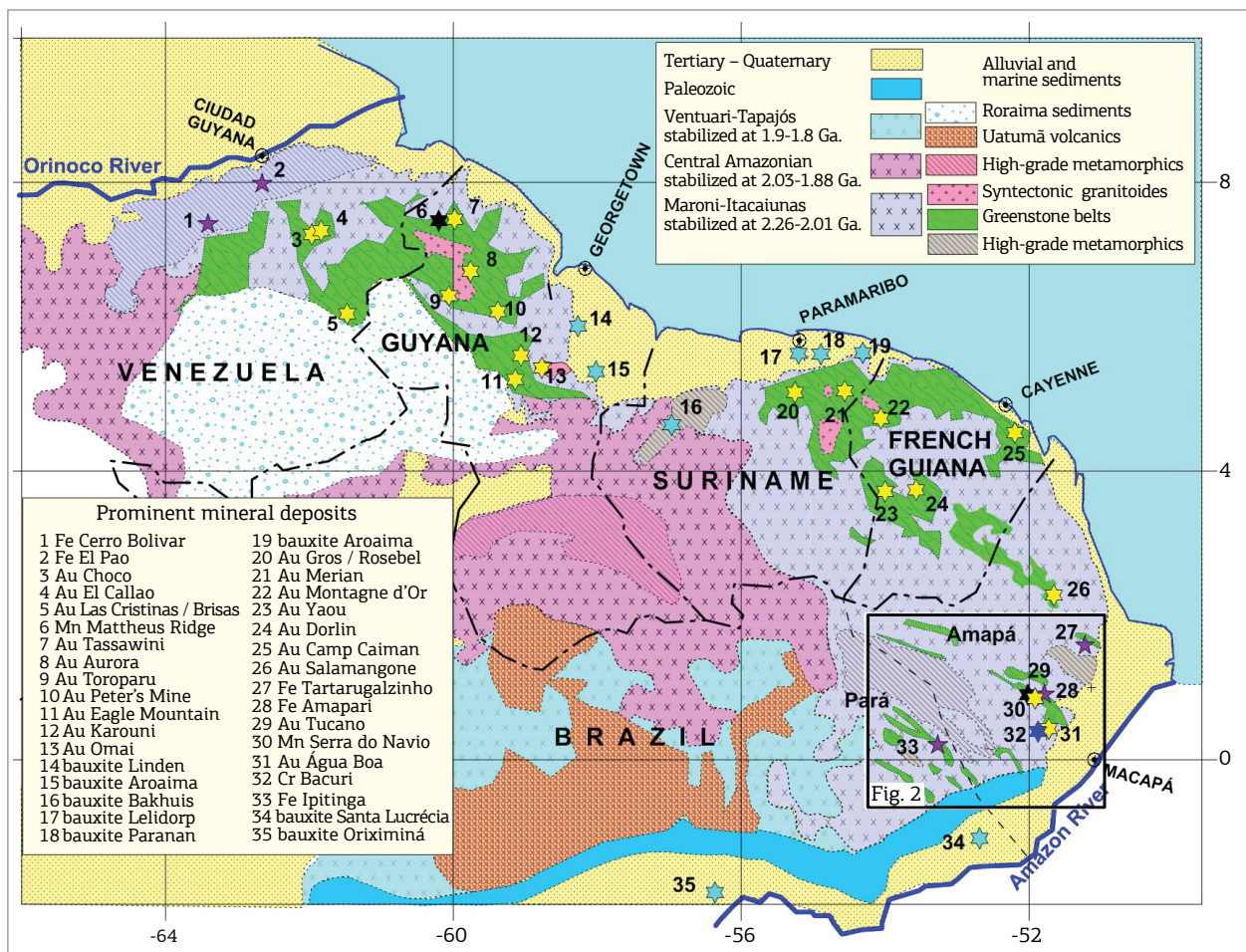


Figure 1. Tectonic Provinces of the Guiana Shield, as presented by the Tectonic Map of South America (Cordani *et al.* 2016), and their main mineral deposits.

marginal arcs, sediments and intrusives. Further west, completing the shield, the Rio Negro-Juruena Province is made of volcano-sedimentary sequences and intrusives related to rift structures and platform sedimentation, altogether stabilized at 1.8 to 1.6 Ga.

This work relates to the Brazilian part of the MI Province north of the Amazon River, in the states of Amapá and Pará. The greenstone belts of this portion of the province, composed by lithologies of the Vila Nova Group, were studied in detail where they host valuable deposits of manganese, iron and gold. Outside of these areas, the deep weathering and lack of outcrops make their study quite difficult.

The name came from the Vila Nova River, site of the first discovery of iron ore in the state of Amapá, in the 1940s. Since then, the exploration of the belts by mine companies were directed essentially to manganese and iron, with individual miners (*garimpeiros*) exploring for gold, cassiterite and tantalite. It was only at about the 1980s that some mine companies started to develop an interest for gold.

Where studied in detail, the Vila Nova Group was seen constituted by metamorphosed volcanic and sedimentary rocks, presenting iron formation in the sequence.

The basement for the greenstones is made of gneisses, migmatites and intrusive granites, granodiorites, and a few diorites. The scarcity of outcrops, allied to the present lack of economic attractiveness of these rocks, leaves them poorly investigated. Their characterization is made mostly from outcrops along river valleys, supported by aerial imagery and aerogeophysical data. Geochronological studies observed a mix of Archean to Paleoproterozoic ages, with some of the Paleoproterozoic rocks representing reworking of Archean protoliths.

Intensive campaigns of regional geological reconnaissance done by ICOMI and other mine companies, looking for manganese and iron formation, revealed the extent of occurrences of manganese oxides and iron formation in the greenstone belts of the MI Province, which is shown in Figure 2. Indeed, they do not occur at random, but are quite limited to well outlined areas and belts, what gives a hint of the extent and continuity of the environments of their deposition. The occurrences of iron formation appear in a 350 kilometers long and 100 kilometers wide belt oriented to northeast, and still open to northeast, to the coast. The good definition of this belt seems to represent

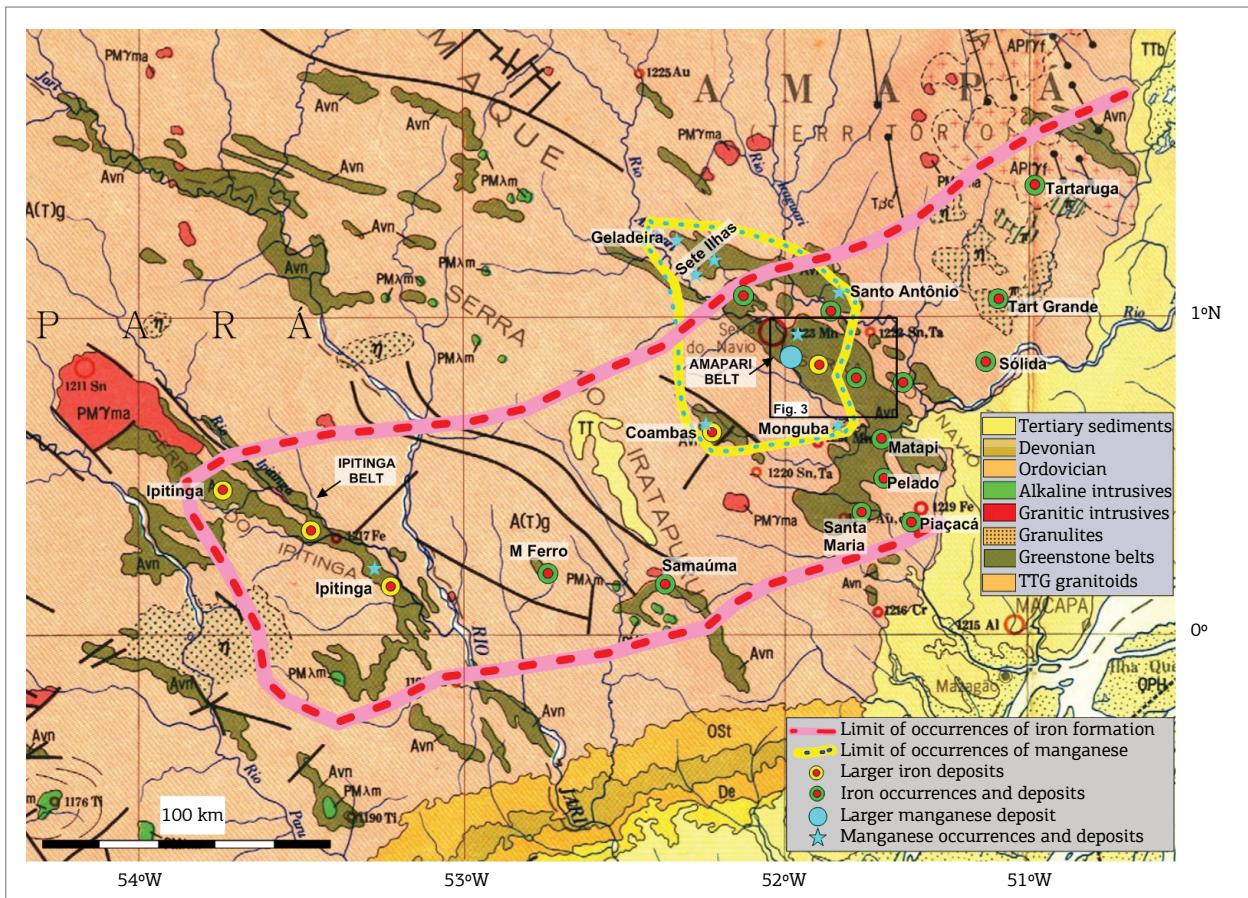


Figure 2. Depository areas of manganese and iron-rich sediments of the Vila Nova Group greenstones in the States of Pará and Amapá, outlined over the Geologic Map of Brazil at 1:2,500,000 (Schobbenhaus et al. 2001).

the depository area of the iron formations. By their side, the occurrences of manganese cluster at about Serra do Navio, at the center-north of the iron-bearing belt, in a situation which possibly indicates the center of the initial deposition of the sediments of the Vila Nova Group.

The greater greenstone belt of the area, the Amapari, at right of center of Figure 2, contains the larger known deposits of manganese, gold and iron, and is also intruded by mafic-ultramafic complexes with the Bacuri deposits of chromite in Santa Maria (Fig. 2), detailed by Spier and Ferreira Filho (2001). The next larger belt, the Ipitinga, at west, is known to contain large resources of iron formation, gold mineralization and showings of manganese.

While these greenstones have most fold axis and regional foliation to northwest, they have large portions with lithological continuity to northeast, along adjacent folded areas, as seen at the southern limits of the Amapari and Ipitinga greenstone belts. This direction to northeast is in good agreement with the orientation of the possible depository area of iron formation, and suggests a previous fold axis in that direction.

In the following items, this article covers of the regional geology of the area of Serra do Navio, Amapá, shown in Figure

3. The Jornal, Serra do Navio and Serra da Canga Formations will be characterized, as well as the Canga and Bicicleta mafic-ultramafic layered intrusions, and the syntectonic granitic intrusions. Later, the larger mines of manganese, gold and iron, where the Vila Nova Group was better studied, will be dealt with from the historical, as well as the geological and technical sides.

REGIONAL GEOLOGY OF SERRA DO NAVIO

In the Amapari Greenstone Belt, the Vila Nova Group is composed by one sequence of mafic metavolcanics, the Jornal Formation, outcropping at southwest, and two sequences of metasediments marked by topographic ridges, the Serra do Navio and the Serra da Canga Formations. These sequences are intruded by syntectonic granitic stocks, which form a low-land topography between the ridges (Tab. 1).

The basement of the greenstone outcrops at southwest and northeast of the area. It is made of biotite and/or hornblende gneisses and their foliation is parallel to the foliation of the greenstone.

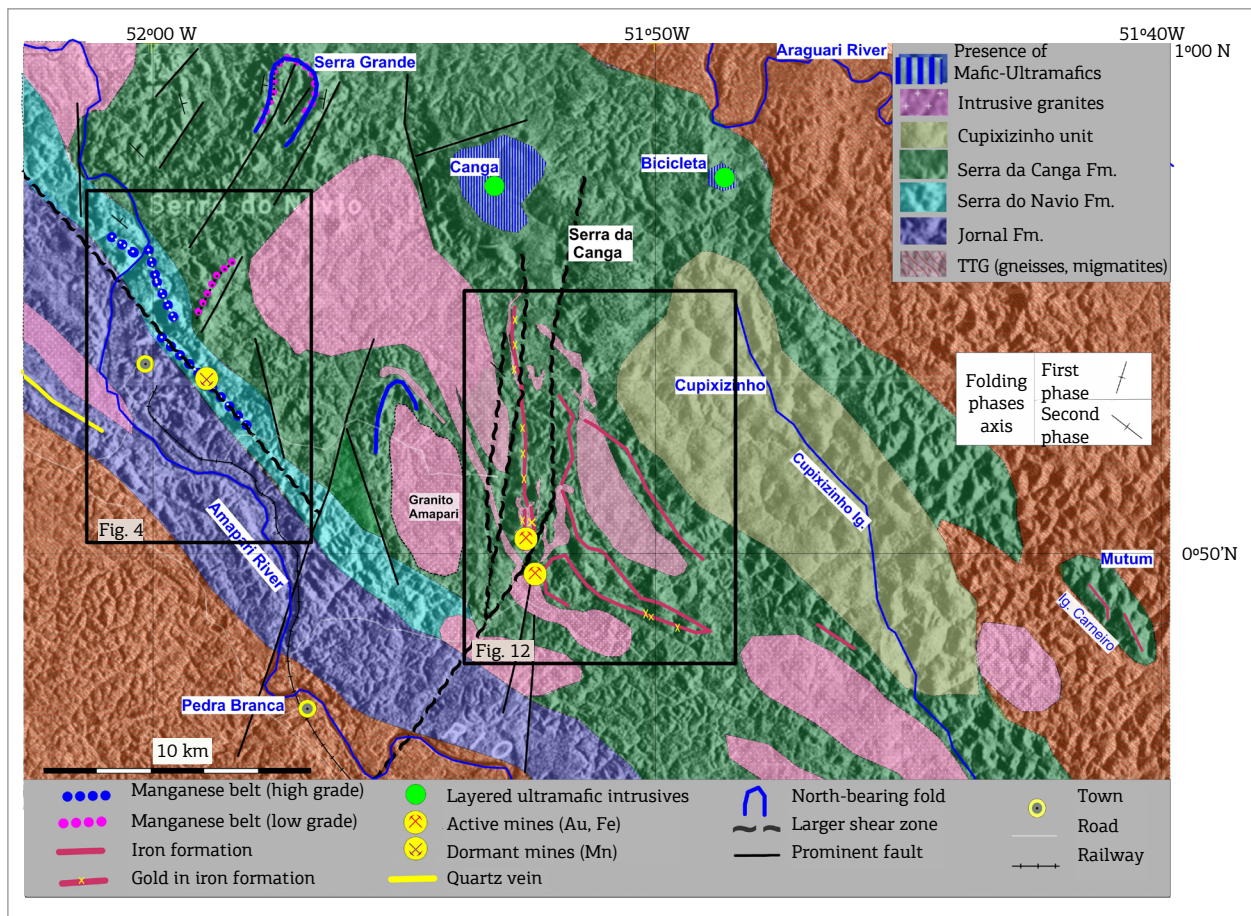


Figure 3. Geology of east of Serra do Navio, with mines of gold, iron and manganese. Presented over the radar image of Projeto Radam (Lima et al. 1976).

Covering the gneisses, the Jornal Formation is made of a more than three kilometers thick pile of orthoamphibolites (defined and formerly named as a group by Nagell 1962, Scarpelli 1966), derived from basalts, but not preserving remnants of the former igneous textures and structures. They are constituted essentially by hornblende and plagioclase (andesine-oligoclase), always containing quartz and magnetite, and accompanied by accessory titanite, epidote, apatite, biotite and other minerals. They are of medium grain size, massive with a weak layering, and with a nematoblastic texture marked by a constant orientation and dip to northwest of the prisms of hornblende. The unit is regionally quite extensive, appearing as the Paramaka Formation in French Guiana, Suriname and Guyana.

Saussuritization of plagioclase and chloritization of hornblende are seen at shear and fault zones. A good example of such retrograde metamorphism into a chlorite schists is seen at the rapids of the Amapari River west of the C5 manganese mine (Fig. 4), where the formation is traversed by the shear zone that follows the T6, T4 and T20 manganese deposits.

At a few sites, the Jornal Formation contains lenses of quartz-mica schists in its basal portion. One of these occurs at west of Serra do Navio. There, a lens of schist extends for a few tens of kilometers to northwest, being marked by a 12 kilometers long ridge parallel to its foliation and made of a fine-grained pyrite-bearing quartz vein or metachert. There is no information regarding the origin of these schists, if metasediments or metavolcanics.

The Serra do Navio and the Serra da Canga Formations overlay the Jornal Formation. Both are made of fine clastic material and chemical components, represented by carbonates, chert and iron oxides, all metamorphosed to the Amphibolite Facies, with local retrograde metamorphism into the Greenschist Facies along a few fractures, faults and shear zones.

These metasedimentary sequences are better known in the areas of the mines of manganese, iron and gold, due to

intense drilling, opening of excavations, geological mapping, and geophysical and geochemical surveys. Other areas of the Vila Nova Group have not so much material for study.

The laterally extensive area of occurrence of these sediments, together with the abundance of carbonates and

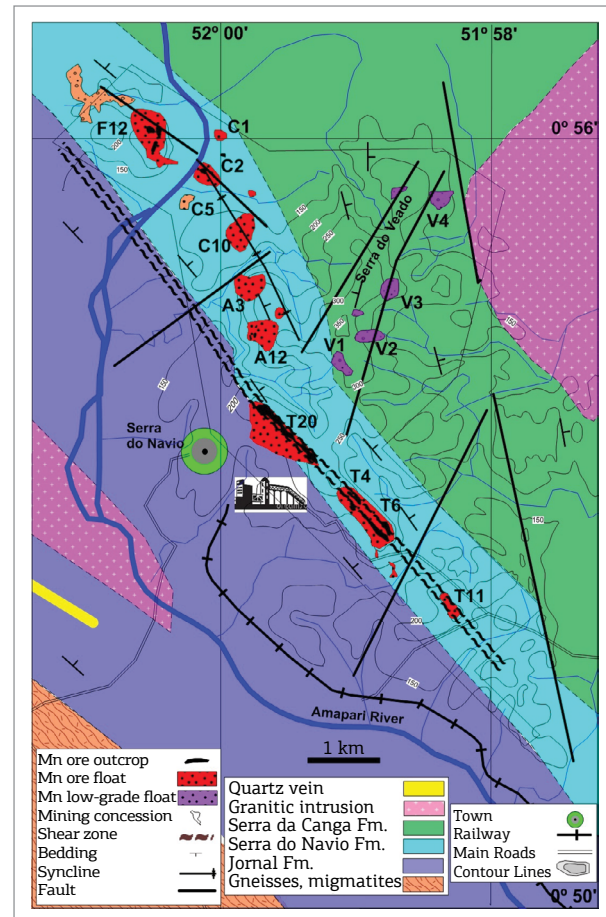


Figure 4. Geologic map of Serra do Navio with deposits and occurrences of manganese of the Serra do Navio and Serra da Canga Formations.

Table 1. Stratigraphic column at Serra do Navio.

| Age | Unit | | Lithologies | Mineralization |
|------------------------------|-----------------------------|---------------------------|--|-------------------------|
| Quaternary | | | Stream sediments | Au, Sn, Ta |
| Triassic | Cassiporé | | Diabase dikes | |
| Paleo-proterozoic | Intrusive layered complexes | Canga | Mafic-ultramafic layered complexes | Possible Cr, Ni, PGE |
| | | Bicicleta | | |
| | Syntectonic acid intrusives | | Granites, monzogranites, granodiorites | Sn and Nb/Ta pegmatites |
| | Vila Nova Group | Serra da Canga Fm. | Platform marine metasediments | Fe, Au, Mn |
| Serra do Navio Fm. | | Littoral/marine cyclothem | Mn | |
| Jornal Fm. | | Orthoamphibolites | | |
| Paleo-proterozoic to Archean | Basement | | Gneisses, migmatites, granitoids | |

chert, the alternation of layers, and the absence of coarse and medium grained sediments, suggests that they were deposited on a marine platform, with presence of littoral facies. Their layers have distinct composition and appear with thicknesses varying from centimeters to meters, with granulometry varying from fine to medium grained. Those derived from pelitic sediments have more micaceous minerals (biotite, muscovite, chlorite, graphite), and are better foliated. Layers derived from quartzous and chemical sediments are more uniform and massive, lacking a good foliation, appearing as quartzites, marbles, manganese marbles, metachert, and banded iron formations. Amidst these end-terms, there are layers with intermediate compositions and textures.

Lafon *et al.* (2008) report Sm-Nd ages of 2.23 Ga. for orthoamphibolites of the Jornal Formation and schists of the Serra do Navio Formation, and Pb-Pb ages of 2.21-2.25 Ga. for syntectonic granites intrusive in the greenstones. These ages correspond to the 2.18-2.09 Ga. period indicated by Kroonenberg *et al.* (2016) for the first phase of the Transamazonian Orogeny in Suriname, expressed in the Marowijne Greenstone Belt by ocean floor magmatism, volcanic arc development, sedimentation and metamorphism, accompanied by some anatexis and plutonism, a sequence of events that agrees with what is seen at Central Amapá.

The Amapari Greenstone Belt was actually affected by two phases of dynamothermal metamorphism, and between them there was one phase of thermal metamorphism caused by the syntectonic granitic intrusions (Scarpelli 1973, Chisonga *et al.* 2012). Before the second dynamothermal metamorphism, the Vila Nova Group was also intruded by a few layered mafic-ultramafic complexes (Horikava & Ferreira Filho 2003).

Common porphyries, like garnets, were formed during both phases of dynamothermal metamorphism. Porphyroblasts formed during the thermal metamorphic episode are common, varying in composition and size depending on the composition and resistance of the host. Skarn-style porphyroblasts are frequent in carbonatic rocks near the granitic intrusives. Quite often, porphyroblasts preserve in their interior remnant minerals of the first metamorphic phase.

During both dynamothermal metamorphisms, the group was folded into synclines, which are the most typical structure of greenstone belts, with anticlines only observed at areas of complex structures caused by faults and shear zones, or in domes formed by uprising syntectonic granitic intrusions. As indicated in Figure 3, while the second folding phase has their axis to northwest, the first one has axis oriented to north-northeast, as indicated by the extensions of the Amapari and Ipitanga greenstone belts to southeast at their

southern extremities, and remnant folds axis to north-northeast, as seen at Serra Grande, north of Serra do Navio.

The shape of the greenstone belts, style of the major and minor folds and the dips of the beds, suggests that the pressure during the first tectonic phase came from the east, while during the second came from the northeast. The metamorphic grade in the second phase reached the Amphibolite Facies. Retrograde metamorphism occurred in less competent lithologies and in zones affected by shears and faults.

Corresponding to the two phases of dynamothermal metamorphism, there are two main directions of shearing, the older to north-northeast and the younger to northwest, both following the main extension of the belts at the time they were formed. The shears to northwest are remarkably longer than the other shears and might correspond to the Transamazonian tectonic event. They are characterized by lineaments with complex tectonic structures, recrystallization and, frequently, by faint to strong hydrothermalism and retrograde metamorphism, marked by chlorite, carbonates, sulfides, epidote, tourmaline, and quartz veins and veinlets.

Some of the shears oriented north-northeast seem to constitute structures of the first dynamothermal metamorphism, reactivated in the second, and have the affected layers subparallel to them. Being oblique to the stress field of the second phase of folding, they constituted areas of pressure release, and as such became favorable sites for appearance of open spaces used as channel ways for hydrothermal solutions. In effect, north-south shears control the most important hydrothermal mineralization observed in the region.

The Paleoproterozoic syntectonic granitic intrusives are quartz-feldspathic, coarse grained, presenting muscovite and poor on femic minerals. Quite often, they have flakes of muscovite oriented parallel to the foliation of the greenstone rocks. Pegmatites intrude adjacent schists and some are mineralized in cassiterite and/or tantalite.

At Serra da Canga there are a few layered mafic-ultramafic intrusives, covered by several meters thick canga cap (lateritic duricrust). Their presence is indicated or suggested by the greater thickness of canga, scarcity of residual quartz and micas in the canga, and by magnetic anomalies.

Triassic diabase dikes related to the Central Atlantic Magmatic Province (Marzoli *et al.* 1999) are quite common in the area, but not marked in the map. They usually form straight and long magnetic anomalies and on surface are recognized by floats of diabase and a dark brown soil. Most of them strikes to north and northwest and has thickness of a few to hundreds of meters.

Alluvial deposits accumulate in the valleys of the area. Some are exploited by *garimpeiros* and small mine companies for gold, and for cassiterite and columbo-tantalite derived by erosion from near-by pegmatites.

THE SERRA DO NAVIO FORMATION

The Serra do Navio Formation, in sharp contact with the orthoamphibolites of the Jornal Formation (Figs. 3 and 4), is constituted by a cyclothem of fine-grained clastic and chemical sediments containing lenses of calcite marbles and rhodochrosite marbles (Scarpelli 1973), the latter constituting the protore of the mined out high-grade manganese-oxide orebodies (Nagell & Silva 1960, Nagell 1962). The formation is covered at northeast by the Serra da Canga Formation.

The cyclothem is shown in Figure 5, with transversal and longitudinal cross sections of the C2 mine, one of the deposits less affected tectonically. Three cycles were exposed there, each cycle starting with an oxide facies at base, covered by a pelitic zone and ending up with a facies of reduction (Scarpelli 1966, 1973).

The oxide facies is represented by cherts, lenses and disseminations of calcium carbonates, claystones and possibly also siltstones, metamorphosed to siliceous to carbonatic schists and limestones. The facies appears as alternating layers of muscovite quartzites, metacherts, plagioclase-muscovite-biotite-quartz schists, calc-silicate schists, tremolite-carbonate schists and marbles. The grain size varies from fine in the cherty layers to medium and coarse in the calc-silicatic units. The original layering is well preserved due to the differences of composition of the individual layers, and frequently the foliation expressed by the micaceous minerals cut across the layering.

The intermediate facies is formed by metapelites metamorphosed to a medium grained garnet(almandine)-biotite-quartz schists, in which the foliation is good and the original layering is usually difficult to recognize.

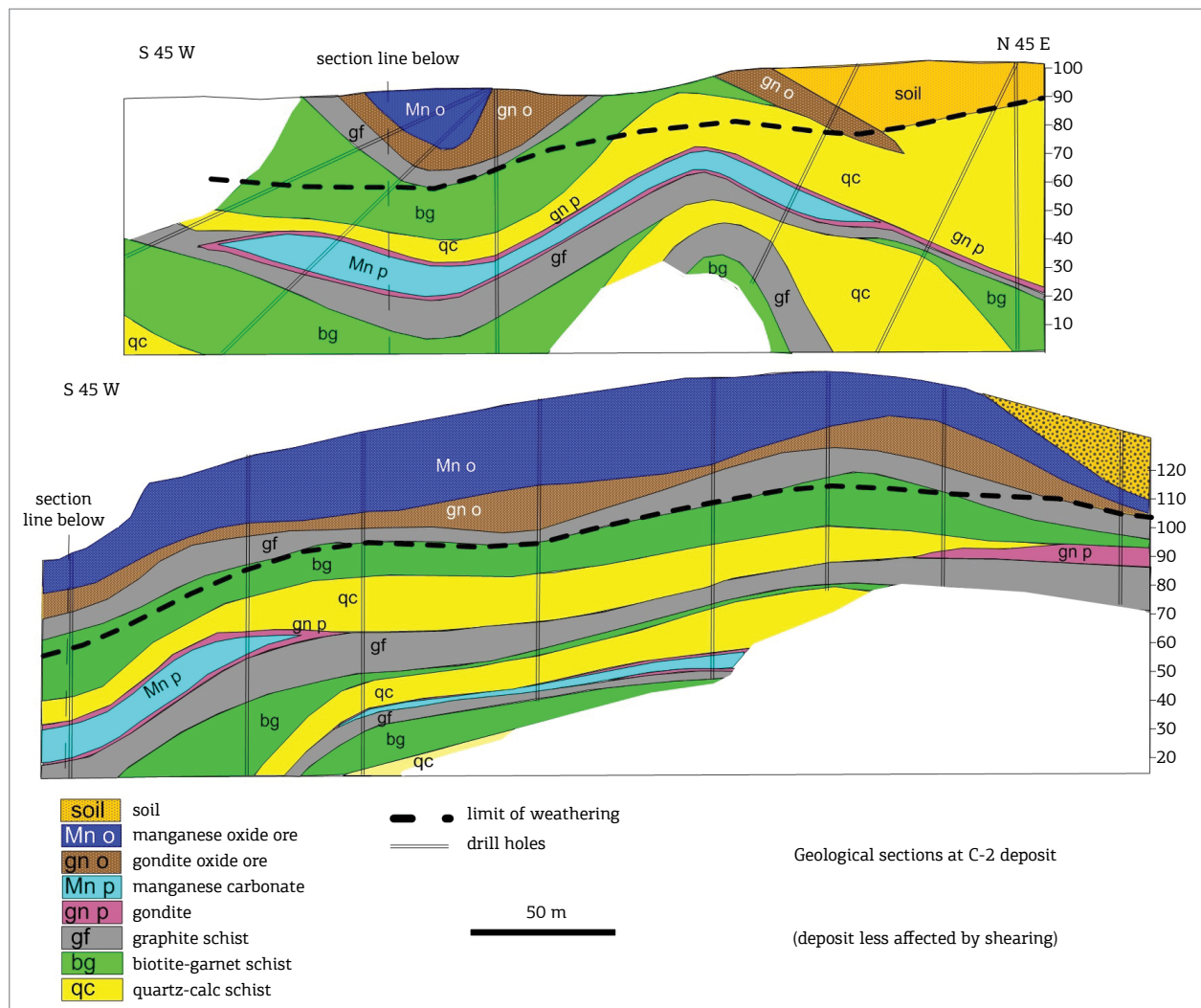


Figure 5. Serra do Navio Formation cyclothem in longitudinal and transversal sections of the C2 deposit (Scarpelli 1972).

The facies of reduction was a pelite rich in organic matter, locally with a transition to a lens of manganeseiferous carbonate near the top. The pelite was metamorphosed into fine-grained quartz-biotite-graphite schists, and the lenses of manganeseiferous carbonates to spessartite-rhodochrosite marbles, also containing pyroxmangite, picrotrophite, rhodonite and other silicates of manganese (Silva *et al.* 1963). The transition zones between the pelites and the manganeseiferous carbonates were metamorphosed into gondites (Leinz 1948), a coarse-grained rock made of spessartite, silicates of manganese, graphite and quartz. The garnets of the manganese marbles have less than one millimeter of diameter, and appear isolated in abundant ground mass, while those of gondites are greater, usually or more than 2 millimeters, and are more abundant, packed one to another. Under weathering the manganese marbles are oxidized to high-grade manganese ores and the gondites to low-grade ores.

The deposition of the cycles seems to have occurred at the littoral zone of a stable marine platform, and was repeated due to advances-and-retreats of the sea level. Each cycle was initiated under open sea conditions, with deposition of the calcium carbonates, chert, and silty and pelitic materials, an environment typical of oxide facies sedimentation. With a decrease of the water depth, the deposition of chemical sediments slowly decreased and eventually ceased altogether, with only clays being deposited. With further decrease of the water depth, the environment became somewhat stagnant, swampy, and the sediments became rich in organic matter, an environment typical of reducing facies. Later in this facies, lagoons appeared and became sites for deposition of the manganeseiferous carbonates (Scarpelli 1966, 1973).

Quite significant, while the sedimentation was changing from oxide to reducing, the contacts between the alternating layers were dominantly transitional. In contrast, the transitions from the upper part of the reducing facies to the oxide phase of the next cycle are always abrupt, indicating rapid raising of the sea level (Scarpelli 1966).

The strong chemical contrast between the oxide and the reducing facies is well expressed by the different conditions required for deposition of carbonates of calcium and of manganese. While the deposition of calcium carbonates requires an environment of oxidation, characteristic of open sea, the deposition of carbonates of manganese requires a restricted and reducing environment. The observation that graphite occurs exclusively in the facies of reduction, in association to the manganese marble, led to the conclusion that the graphite-schists are product of pelites rich in organic matter, a typical product of swampy environments (Scarpelli 1966).

A petrographic study of the lithologies of the cyclothem (Scarpelli 1968) has shown that based on their porphyroblasts and accessory sulfides, they could be divided in five distinct groups (Tab. 2), which seems to reflect their different degrees of competence and even origin. The groups are:

- Muscovite-biotite-quartz schists and metacherts;
- Calc-silicate rocks and associated limestones from the oxide facies;
- Almandine-biotite-quartz schists from the intermediate facies;
- Graphite schists;
- Rhodochrosite marbles and gondites from the facies of reduction.

Andalusite, sillimanite and staurolite, indicators of metamorphic conditions, appear in the silicatic schists with different frequencies, giving a hint about the differential resistance of these rocks to the superposed phases of metamorphism. Usually, the presence of staurolite indicates the higher pressure and temperature of metamorphism (PT), sillimanite an intermediate PT and andalusite the lower PT.

Frequently porphyroblasts that grew during the thermal metamorphism envelop and preserve as inclusions minerals of the first dynamothermal metamorphism, making clear

Table 2. Porphyroblasts and sulfides in the Serra do Navio Formation.

| Depositional Facies | Lithologies | Most Common Porphyroblasts | Accessory Sulfides |
|-----------------------------|--|--|--|
| Reducing (graphitic) | manganeseiferous marbles and gondites | spessartite rhodonite picrotrophite pyroxmangite | niccolite gerdorsffite sphalerite cobaltite |
| | graphite schists | andalusite >> sillimanite sillimanite >> staurolite | pyrite > chalcopyrite |
| Neutral (biotitic) | almandine-biotite-quartz schists | almandine sillimanite >> andalusite = cordierite | pyrite >> chalcopyrite |
| Oxide (quartzous, calcitic) | limestones, cherts and calc-silicate schists | diopside tremolite grossularite | pyrrhotite > arsenopyrite |
| | muscovite-biotite-quartz schists, quartzites | almandine sillimanite >> andalusite andalusite >> staurolite | pyrrhotite |

the differences in structural orientation of the two phases of dynamic metamorphism (Fig. 6A).

Quartzous schists, usually less ductile and more resistant to the metamorphic stresses, are the favorite host for staurolite (Fig. 6B), which does not occur in the ductile micaceous schists. The well foliated garnet-biotite-quartz schist of the intermediate facies was quite able to dissipate metamorphic stresses, not appearing with staurolite. It avoided the metamorphic stresses with displacements along the planes of foliation and displacements of its minerals (Figs. 6C and 6D).

In the units rich in calcium carbonates, diopside is the more common porphyroblast, often replaced in total or at the edges by tremolite during the second dynamic metamorphism.

In the manganese marbles, very often there are crystals of rhodonite (MnSiO_3) and/or picrotremolite ($(\text{Mn,Mg})_3\text{SiO}_4$), occasionally one replacing the other. These replacements are usually seen where the rock is fractured and where adjacent

non-carbonatic rocks present veinlets of quartz, which are never seen crossing the manganese marbles. Considering that picrotremolite is unsaturated in silica in respect to rhodonite, the formation of one or the other might have been dependent of the volume of silica available during the crystallization of the mineral. In such a way, more silica would lead to rhodonite instead of picrotremolite, and vice-versa (Scarpelli 1966).

All rock samples of the cyclothem present accessory sulfides, which are distinct for each rock group. Samples of the rhodochrosite marbles showed, without exception, presence of sphalerite, niccolite, cobaltite and gersdorffite, suggesting a close relation with the orthoamphibolites of the footwall Jornal Formation. The graphite and the biotite schists appear with pyrite and occasional chalcopyrite; the metacherts present arsenopyrite; the marbles, calc-silicate schists and associated quartzites contains pyrrhotite; and galena was seen in

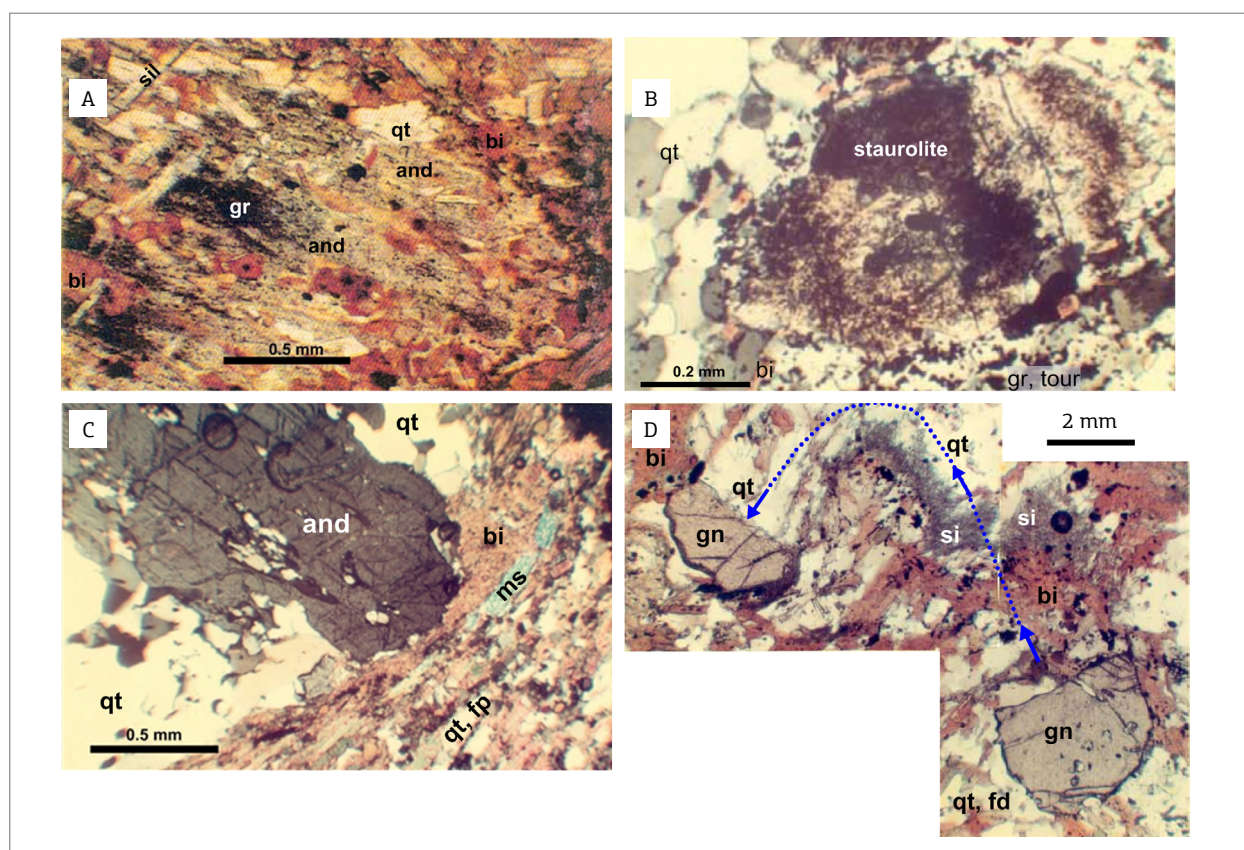


Figure 6. (A) Andalusite (and) porphyroblast preserving lines of grains of graphite (gr), remnants of the first dynamothermal metamorphism. Sillimanite needles (sil), and biotite (bi) plates, formed during the second dynamothermal metamorphism, replace andalusite. (Mine C-2, hole 42, 41 m). (B) Twinned staurolite in quartzous graphitic schist; biotite, quartz; graphite and tourmaline (tour). (Xnicols, mine T4, hole 30, 84.5 m). (C) Garnet-biotite-quartz schist with andalusite porphyroblast rotated to 90° of foliation. Pressure-free areas at both sides of the porphyroblast are filled with quartz. Biotite and muscovite (ms), and feldspar (fd). (Xnicols, mine T-20 hole 15, 86 m). (D) Biotite-garnet-quartz schist with an almandine garnet (gn) broken in two fragments during the second dynamothermal metamorphism, with one of them pushed along a curved path, up and to the left in the figure. Clouds of sillimanite needles formed where the moving half garnet pressured and heated the rock along its path, while quartz filled the zone of low pressure behind it. (Mine C5, hole 2, 75 m). (Scarpelli 1969)

a few quartz veins. Most of the sulfide grains occur disseminated in the rocks, but some were remobilized into veinlets.

Both the manganese marbles and the associated gongdites constituted protodes for the oxide ores of manganese, described ahead.

THE SERRA DA CANGA FORMATION

The Serra da Canga Formation directly overlays the Serra do Navio Formation at west and the Jornal Formation at south, and, at north, it is in contact with basement rocks at the Rio Araguari (Figs. 3 and 4). The formation is well exposed at Serra da Canga, 15 kilometers to the east of Serra do Navio, after a lowland area with syntectonic granites. The Serra da Canga itself is marked by a prominent plateau at the elevation of about 250 meters above sea level, covered by a more than 8 meters thick cap of canga, an indurated duricrust made of massive limonitic laterite. Leaving the plateau to the south, this cap becomes thinner, with the topography marked by ridges formed by the rocks more resistant to erosion. Although scarce, outcrops of the formation are seen at the flanks of the plateau, and along the valleys between the ridges. The formation was quite well detailed at south of the plateau during the exploration conducted for gold by Unigeo Geologia e Mineração, Minorco Brasil and AngloGold Ashanti, subsequently followed by the exploration for iron done by Min. Pedra Branca. A few drill holes in the plateau revealed two layered mafic-ultramafic sequences intruding the formation.

Lowland topography in the area occupied by the formation marks the presence of syntectonic granitic intrusives.

At Serra do Veado, immediately to the east of the manganese mines of Serra do Navio, the basal part of the formation strikes north, in apparent structural discordancy with the Serra do Navio Formation (Fig. 4). This portion of the formation is constituted by a sequence with paramphibolites at base, covered by quartz-biotite schist, biotite-cummingtonite-actinolite schists, metachert, culminating with quartz-biotite schists containing a layer of gongdite, floats of which accumulate in the areas V-1, V-2, V-3 and V-4. Shallow core holes in these areas revealed a few meters thick layer of oxidized gongdite, with grades of 20 to 30% Mn. Tonnage, grade and content of silica were unattractive for economic exploitation. The gongdite-bearing unit continues to the north, until Serra Grande (Fig. 3), where drilling also indicated low tonnages and similar grades of manganese and silica. Some holes in this area revealed a narrow band of graphite schist next to the gongdite. The paramphibolites below the gongdite-bearing horizon are composed of quartz, hornblende, actinolite, plagioclase, clinzoisite, plus minor percentages of biotite, chlorite, greenish diopside, epidote, carbonate, and other minerals. Contrasting with the orthoamphibolites, they are mineralogically well layered, lack the massive nematoblastic texture that characterize the orthoamphibolites, and magnetite is hardly seen. The sequence is considered to represent metamorphosed marls, deposited on calm marine platform. The formation suffered the same metamorphic phases observed with the Serra do Navio Formation.

Table 3. Stratigraphic Column of Serra da Canga Formation.

| Unit | Characteristic | Lithology |
|----------------------------------|---|--|
| Clasto-Pelitic Metasediments | Sandy Domain | Fine-grained quartzites: muscovite quartzites, muscovite-quartz schists, muscovite quartzites with fuchsite and/or sillimanite |
| Clasto-(Chemical) Metasediments | Pelitic Domain | Mica schists: quartz-mica schists, garnet-quartz-biotite-muscovite schists, lenses of calc-silicatic rocks and iron formation |
| | Transitional | Quartz-grunerite-cummingtonite schists, quartz-amphibole schists, lenses of iron formation and calc-silicatic rocks |
| (Clasto)- Chemical Metasediments | Ferrous Domain | Silicatic iron formation: magnetite-grunerite-hornblende schists, garnet-hornblende-grunerite-diopside, |
| | | Oxide iron formation: coarse grained banded iron formation, with quartz, magnetite and grunerite and occasional garnets; fine-grained banded iron formation with quartz and hematite |
| | | Silicatic iron formation: foliated to banded magnetite iron formation with grunerite and hornblende, and occasional diopside and lenses of marble |
| | Calcic Magnesian Domain | Diopside calc-silicate rock; unfoliated rock with coarse grained diopside, plus calcite, quartz, actinolite; lenses of iron formation |
| | | Calcic-magnesian-silicate schists; foliated rock with hornblende, actinolite, diopside, magnetite, calcite, quartz, forsterite; lenses of marble |
| Manganese Horizon | Marbles and carbonate schists: marble, carbonate schists with serpentine replacing olivine, actinolite, tremolite, diopside, forsterite, fayalite, hastingsite, cummingtonite, chlorite and magnetite | |
| Base | Metamarls, Basic Metavolcanics | Gongdite or manganese-bearing schist, with/without a thin layer of graphite schist |
| | | Paramphibolites; banded paramphibolites Basic meta-volcanics; amphibole schists with cummingtonite, hornblende, biotite and magnetite, remnants of igneous textures. |

As shown in Table 3, above a basal section of amphibole schists and amphibolites, the sequence becomes essentially clasto-chemical, with a manganese-bearing unit at the base, changing upwards to calcic, to magnesian and to iron domains. The rocks of the Calcic-Magnesian Domain (Fig. 7), and the Ferrous Domain (Fig. 8), are marked by silicates of calcium, magnesium and iron, as diopside, tremolite, actinolite, serpentine, fayalite, forsterite, cummingtonite, grunerite, garnets and others, frequently accompanied by magnetite and sulfides of iron. Layers of metachert are seen all throughout the sequence. At the upper part of the Ferrous Domain, after a fine-grained massive sillimanite quartzite, possibly a metachert, the chemical components diminish, and the formation becomes dominated by metapelites and metasiltites, metamorphosed into quartz-mica schists and garnet-quartz-biotite-muscovite schists, with occasional lenses of calc-silicatic rocks and silicatic iron formation.

Quite important economically, the Ferrous Domain is marked by layers of silicatic and oxide banded iron formations, which, besides quartz and iron oxides, contain silicates of iron, magnesium and calcium, often accompanied

by carbonates. The composition of the iron formation changes according to their position in the stratigraphy and the area of occurrence. The more common types, from the base to the top of the sequence, are those noted ahead (Horikava 2008):

- Bif 1: Greenish gray and fine to medium grained, highly magnetic, composed mostly by bands of magnetite and quartz, containing diopside, locally with grunerite and occasional hematite;
- Bif 2: Darker than Bif 1, it is highly magnetic and made of bands of magnetite and quartz containing silicates, amongst which garnets (andradite and grossularite) and grunerite and hornblende predominating over diopside. In hydrothermally altered areas, they present pyrrhotite and pyrite in masses or in thin bands concordant to the layering (Fig. 8);
- Bif 3: Intermediate to Bif 1 and Bif 2 in color and silicate content, it presents bands of hematite in addition to those of magnetite;
- Bif 4: Bands of hematite and quartz, frequently with diopside, predominate over bands of magnetite. Locally resemble itabirites (Fig. 8).

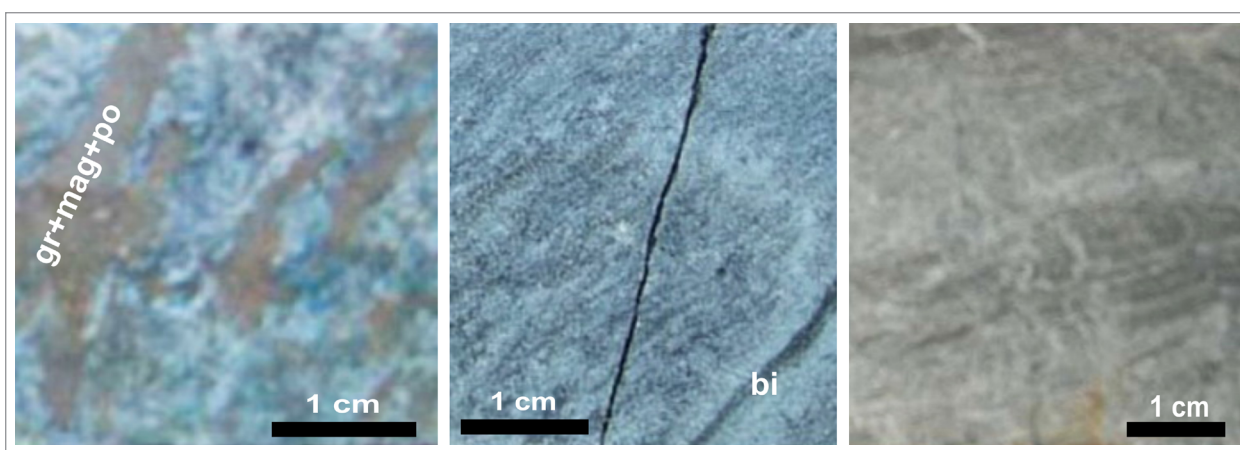


Figure 7. Calcic-Magnesian Domain. Left: Impure and weakly foliated marble, with serpentine, brown grunerite, magnetite and pyrrhotite. Center: Carbonates, diopside, grunerite, with biotite in bands. Right: Impure marble with fine grained diopside

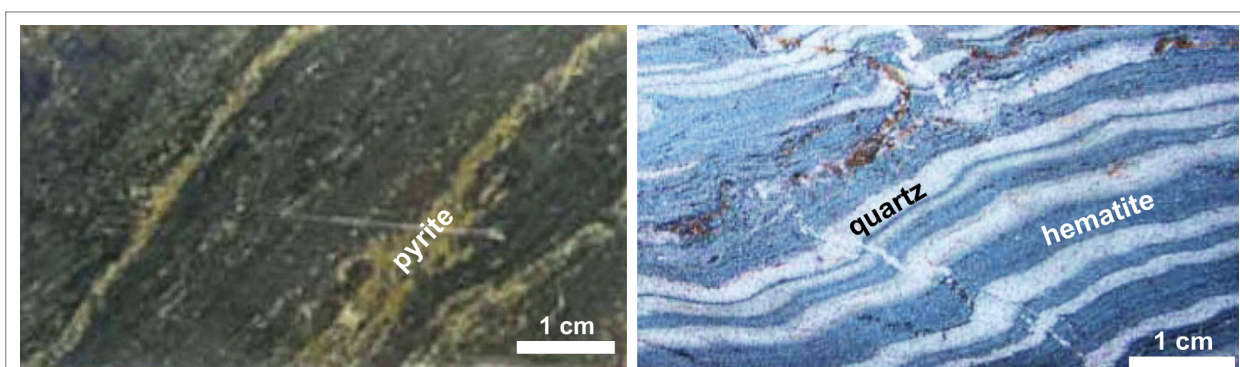


Figure 8. Ferrous Domain. Bif 2, at left, with lighter bands of quartz, grunerite and diopside alternating with darker bands of magnetite, hornblende, and grunerite; yellowish bands are rich in pyrite. Bif 4, at right, formed essentially by bands of hematite and quartz. Units of Bif 4 are more common in the area mined for iron.

The clastic domain is better developed southeast of Serra da Canga, in the basin of the Cupixizinho River (Fig. 3). This area is poorly known, with the available information restricted to observations from scout exploration lines, limited soil geochemistry, aerophotogeology and aerogeophysics. From what it is known, ridges of fine-grained quartzites and quartz-mica schists dominates the area, with lines of banded iron formation flanking it by the southwest and northeast. The area is crossed by a few shear zones, the greater following the valley of the Cupixizinho River.

The area with the present gold and iron mines is shown in Fig. 9, which emphasizes the unit of iron formation that hosts the deposits. At east, the structures strike to northwest, characteristic of the second dynamothermal metamorphism, being highly deformed along a north-south shear zone, along which the beds, initially striking northwest, assumed a north-south strike, concordant to the shear and the granite at west.

This shear zone seems to have been formed during the first dynamothermal metamorphism, just reactivated in the second. It strongly affected the Serra da Canga Formation, steepening, fracturing and faulting the beds, and its strike, oblique

in relation to the regional compression from the northeast, favored the appearance of open spaces used by the ascending hydrothermal solutions. The gold mineralization is about continuous along the 8 kilometers of iron formation paralleled to the shear, from Urucum to Tap AB1 and Torres.

Woodpecker, Duck Head and Gold Nose, important gold deposits in the iron formation, occur at the southern limb of the syncline east of Taboca. With the tectonic compression coming from the northeast, this limb was highly compressed and fractured against its footwall, with the fractures oriented to about north constituting good sites for hydrothermal deposition of mineralization.

Gold mineralization also occurs in non-iron formation units, as seen at Tap D, on a wedge of the Calcic-Magnesian Domain at west of the north-south shear. Still preserving the initial strike to northwest and the general dip to northeast, this wedge is composed of carbonatic and calc-silicate schists containing auriferous concentrations of sulfides (pyrite, pyrrhotite, plus chalcopyrite and arsenopyrite), appearing as disseminations and replacements of carbonates and silicates. Nearby, the Unigeo/Minorco soil sampling identified attractive anomalies of copper, lead and zinc which seems to have not been examined yet.

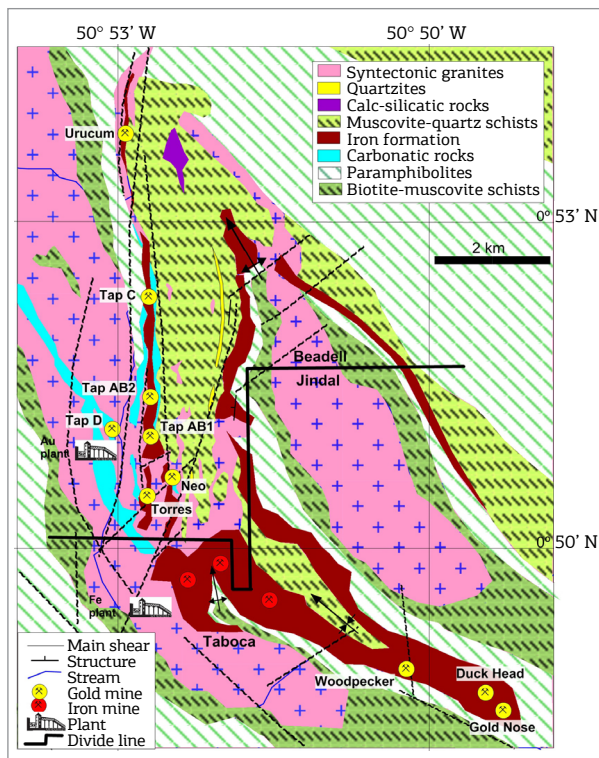


Figure 9. Geology of the area with the gold and iron mines of Beadell and Jindal. The larger gold deposits occur in iron formation, controlled by shears and faults. At west of the major controlling shear, TapD gold deposit occurs in a wedge of the Calcic-Magnesian Domain. Mineral rights of the complete area belongs to Beadell, with Jindal owning rights to exploit iron south of the divide line. (Base geologic map from Horikava E.H. 2008).

CANGA AND BICICLETA: MAFIC-ULTRAMAFIC LAYERED INTRUSIVES

The only rock exposures seen at the Serra da Canga appear at the flanks of the canga covered plateau, in the form of weathered schists and quartzites.

Two scout drilling campaigns were realized on the plateau, one over a magnetic anomaly at Canga, at its northern portion, and the other at Bicicleta, 12 kilometers to the east, over a soil geochemical anomaly of nickel (Fig. 3). Both campaigns revealed metasediments of the Serra da Canga Formation intruded by lithologies corresponding to layered mafic-ultramafic complexes (Horikava & Ferreira Filho 2003). All cored rocks have been metamorphosed to the Amphibolite Facies.

At Canga, the intrusives appeared in 3 out of 13 holes, with intersections of 26, 94 and 120 meters, and their structure was not clearly defined. The hole with 26 meters of intersection exposed a complete section of the intrusion. At base, it presented layers of metaperidotite, passing to metapyroxenite and ending above with layers of metagabbro (Fig. 10). The hole with 94 meters of intersection exposed only metapyroxenite. The hole with 120 meters of intersection missed the upper part of the intrusion. At base, it presents metaperidotites, which are overlain by layered metapyroxenites, that pass upwards into saprolite and canga. The ultramafic rocks present moderate primitive composition, with MgO 18.5-24.7%, Mg No 0.45-0.54, CaO 4.0-9.6% and Cr₂O₃ 0.15-0.18% (Horikava & Ferreira Filho 2003).

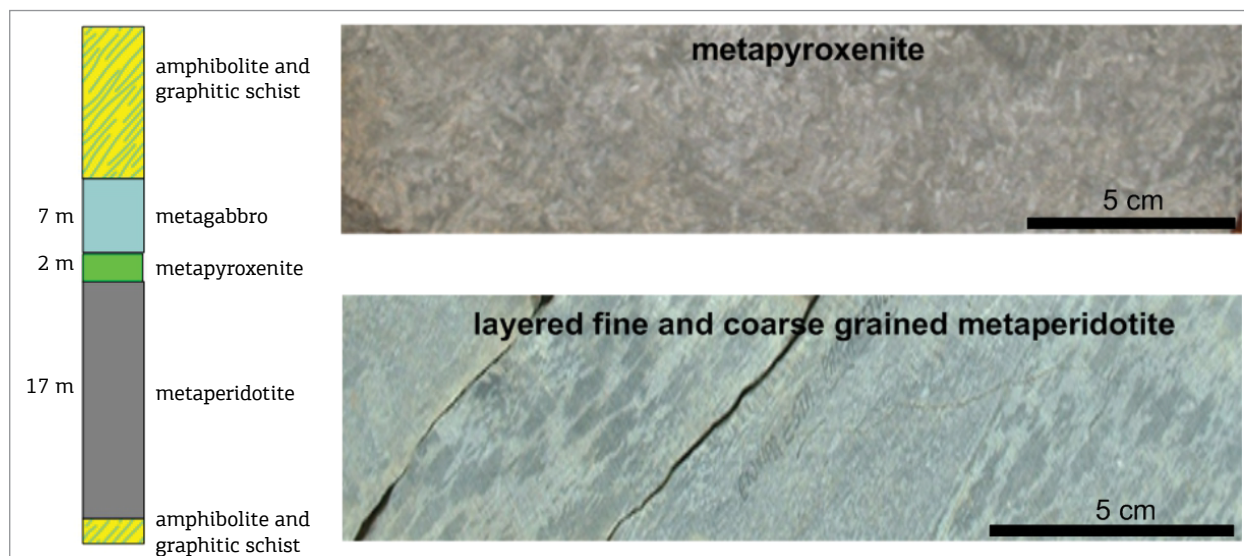


Figure 10. Details of the 26 meters drill intersection of a mafic-ultramafic intrusion in the Serra da Canga Formation at Canga. (From Horikava & Ferreira Filho 2003).

In detail, the basal metaperidotites are formed by alternating layers of olivine, amphiboles (cummingtonite and tremolite) and chlorite. In the transition zone to the overlying pyroxenites there is a foliated olivine tremolite. The metapyroxenite is made of tabular clinopyroxene crystals partial to totally replaced by hornblende. Its transition to metagabbro is marked by small crystals of plagioclase between the tabular clinopyroxene. The metagabbro is made of hornblende and plagioclase in diablastic and nematoblastic textures. The sequence suggests fractionated crystallization, from olivine to olivine + clinopyroxene, to clinopyroxene, and to clinopyroxene + plagioclase.

At Bicicleta, amidst passages of metasediments of the Serra da Canga Formation, four out of eight holes intersected metaperidotites similar to those ones of the Canga area and ortho-amphibolites that seems to represent metamorphosed gabbros.

Horikava and Ferreira Filho (2003) inform that the two sequences present characteristics of layered mafic-ultramafic intrusives, suggesting that they originated from a basic magmatic chamber under differentiation. They suggested that these rocks could host concentrations of nickel, copper, and platinum.

The aerogeophysical map made by Serviço Geológico do Brasil (CPRM) indicates other magnetic anomaly near the drilled areas, suggesting extensions of these intrusions or additional intrusions of the same type.

SYNTECTONIC GRANITIC INTRUSIVES

Several syntectonic granitic masses intrude the greenstone belts, which they tectonically deform, thermal metamorphose

and also intrude with pegmatites. Their composition varies from granites to monzogranites and to granodiorites (Tavares 2009). Most have an elongated form, doming the intruded lithologies, quite often showing a foliation parallel to the foliation of intruded rocks.

Some appear as dikes in fractures and fault planes, as those seen in the shear zone that host the Tucano gold deposit, as shown in Figure 9. Other ones intrude former intrusions, forming large masses as the Silvestre Granite, which is actually composed of several intrusions, of difficult individual definition.

Some of the pegmatites intruded in the metamorphic rocks are mineralized with cassiterite or columbite-tantalite, constituting the source of concentrations of these minerals in streams of the area, intermittently exploited by *garimpeiros*. Historically, the main centers of this mining are the basins of the creeks Jornal and Silvestre, at west of the Tucano gold mines, and also in several creeks at the basin of the Cupixinho River. Sporadically, small mine companies open up a mineralized pegmatite, which they mine for a couple of years. There is no information of about anyone doing a sustained campaign to identify large pegmatites.

MANGANESE ORES OF SERRA DO NAVIO

The manganese ores which occur in the Serra do Navio Formation can be split in two groups, the oxides and hydroxides of manganese and iron, product of weathering and supergene enrichment of the manganese marbles and associated metasediments, and the fresh manganese marbles themselves. Today,

the resources of oxides and hydroxides are about exhausted, but those of carbonates were barely touched. The preferential mining of the oxides and hydroxides was favored by the large market represented by the metallurgical industry, while the carbonates, mined only in the last years of activity of the mine, have a limited market and heavy chemical constraints.

Under the conditions of extreme weathering of the Amazon rainforest, supergene alteration of the Serra do Navio Formation normally reached depths of 50 to 60 meters, surpassing 100 meters in the more carbonatic zones. In the process, minerals were dissolved and the majority of elements were solubilized. Some, as manganese, iron and aluminum, reprecipitated in the form of oxides and hydroxides, in many cases practically *in situ*, replacing the dissolved carbonates, sulfide and silicates. The newly formed minerals are not essentially stable, as there is evidence of a continuous process of dissolution, leaching and reprecipitation, leading to higher and higher concentrations of manganese. At the end, large blocks of massive manganese ores were formed and stayed in the weathered zone, together with clays and other secondary minerals, being fundamental to form ridges where they occur (Dorr *et al.* 1950).

The main manganese minerals formed are cryptomelane, a hydrated potash-bearing manganese oxide, accompanied by pyrolusite, manganite and a few other minerals like lithiophorite (Valarelli 1967), which intermixed

with iron and aluminum oxides and hydroxides constitute the compact masses. Small quantities of metals like zinc, arsenic, cobalt and nickel are retained within the crystalline structure of the manganese and iron oxides and hydroxides.

Figure 11 presents a cross section of the T6 mine, at the southern end of the line of orebodies of Serra do Navio. The structure is complex due to the shear zone that pushed up the ore blocks from northeast.

- The oxide ore, assaying more than 44-48% Mn, result of *in situ* oxidation of the manganese marbles;
- The low grade and silicatic gondite ores derived from oxidation of gondites;
- The schistous ores, formed by impregnation of manganese oxides in graphitic and carbonatic schists;
- The lateritic ore, formed by the accumulation of granzon (surficial supergenic round nodules of iron-manganese hydroxides) and boulders of massive manganese oxide ores at the flanks of the hills;
- The carbonatic protore.

The oxide ore types were exhausted down to the contact with the carbonatic ore, that was not mined.

The exploitation of the manganese ores was done by ICOMI from 1957 to 1998, being interrupted when the resources became small and the production became

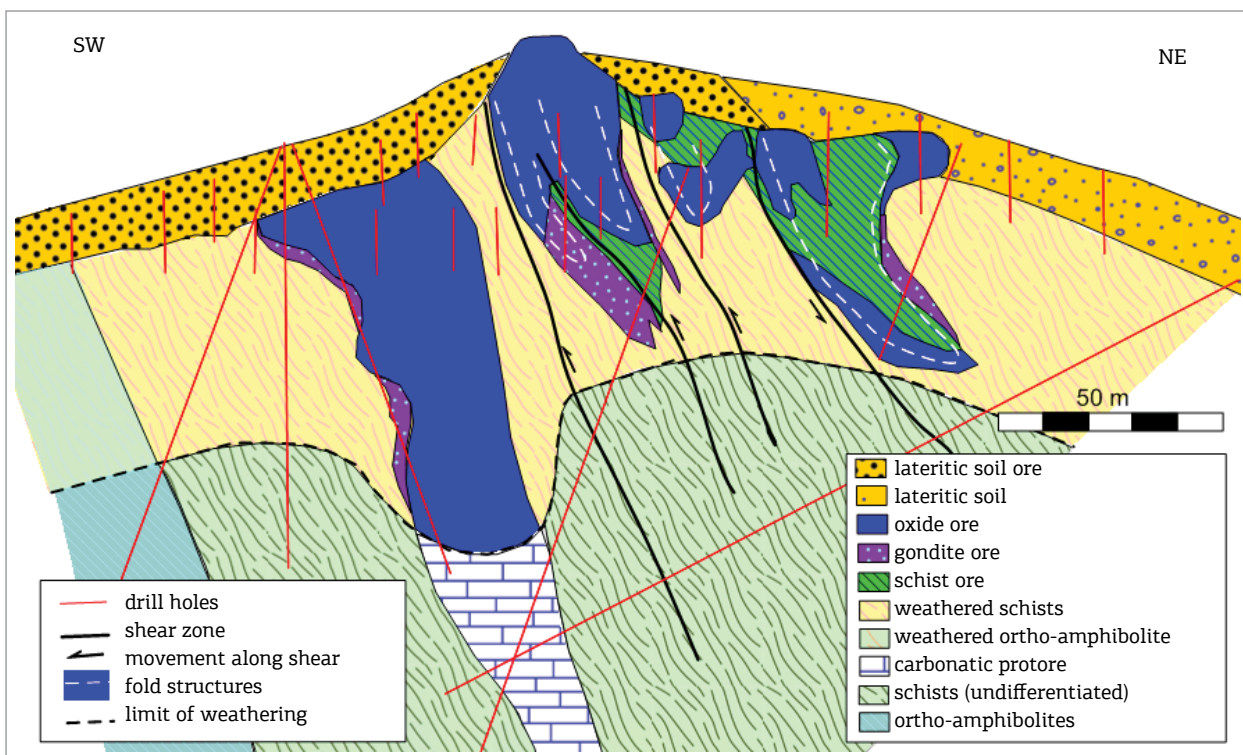


Figure 11. Cross section of the T6 mine, showing effects of the shear zone on structures, depth of weathering and ore types. The oxide ores were mined out.

uneconomical. During its activities, ICOMI sold 31 million tons of washed oxide ore assaying from 42 to 49% Mn, 1.8 million tons of manganese pellets, sinter feed and fines, and 0.9 million ton of carbonate ore assaying about 30% Mn. Most of the carbonate ore produced came from the F12 mine, at the northern end of the line of mines, mostly due to its better topographic situation.

The initial exploration was done with mapping, trenching and drilling. Geologic mapping and additional drilling continued during the life of the mine, to improve the operation and to find reserves to replace the mined tonnage (Marotta et al. 1966). On a few occasions, gravimetry was used to identify deposits hidden below barren ground.

Mining was done in open pits and other surficial excavations. During the opening of the pits, barren and weathered schists at the sides of the ore were stripped off and deposited as waste at the flanks of the hills, which were later recovered with revegetation. For most of the time, the ratio of ore to waste was of about 1 ton of run-of-mine to 1 m³ of waste.

The run-of-mine, constituted by the ore and intervening masses of weathered schists, was sent to a beneficiation plant, where it was crushed, washed and screened. In the process, about 10% of the feed, essentially clays, was eliminated as tailings. The recovered products were constituted by clean fragments of the ore, classified in various commercial sizes. The fragments smaller than 0.8 centimeters were submitted to gravimetric concentration, the coarser of them with dynawhirlpools, set to work at the density of 3 g/cm³, and the finer with Humphrey spirals. In both cases, the lighter fragments were discarded (Rodrigues *et al.* 1986). To improve the commercialization of the recovered fines, a pellet plant was built and operated near the port. For commercial reasons, after some years, this plant was changed to produce sinter feed.

The main constituents of the products were manganese and iron, at a ratio of about 6 to 10:1. It is important to note that this ore contained a very small but important quantity of arsenic, firmly locked in the crystal structures of the ore minerals. The ratio Mn:As was quite stable, at about 3,000:1, that is, an ore product with 48% Mn would have 0.016% As. Metallurgical tests done before the opening of the mine revealed that in the steel industry the arsenic of the ore is not liberated to the air and stays inert, fixed as a metal in the produced steel.

To operate the mine, in the 1950s ICOMI built a 192 kilometers long captive railway from Serra do Navio to Santana, near Macapá, where it built an also captive port. Besides all necessary installations, inclusive a diesel operated power plant for the generation of energy at Serra do Navio, two model villages were constructed for the employees, both with hospital and schools, one at Serra do Navio and another near the port.

Today, while the remaining resources of high-grade oxide ore are negligible, the resources of carbonate ores, which were just touched at the bottom of some of the pits, are there to be considered for underground mining operations, when price and market requirements become attractive. As time goes by, eventually low-grade deposits at the base of the Serra da Canga Formation might become interesting to mine.

When the exploitation was terminated, ICOMI left at surface piles with slightly more than 5 million tons of crushed, washed and classified oxide ore with 17 to 36% Mn, not sold due to a lack of buyers when they were produced, but with a clear chance to be sold at present day conditions. On addition, at the sides of the old pits there are large piles of low-grade resources, made of a mix of schistous and gondite ores and residual clays, roughly averaging 15 to 25% Mn, which could eventually be used to produce saleable products.

GOLD DEPOSITS, THE TUCANO MINE

Gold mineralization in the iron formation was identified and explored by Unigeo and Minorco, both subsidiaries of Anglo American do Brasil, under the name of Amapari Project. It was taken over by AngloGold Ashanti when the Anglo Group split in two, and shortly after it was sold to Mineração Pedra Branca do Amapari Ltda. After commissioning the mine with a heap leach plant and operating it for a while, Min. Pedra Branca sold it to Wheaton Mining, that subsequently sold it to New Gold. In 2010, Beadell Resources Ltd. acquired the project and is keeping it in continuous operation, under the name of Tucano Mine. Due to the local heavy rain conditions, the heap leach process always had problems and, to improve gold recovery, soon after the acquisition Beadell installed a 3.5 million tons per year carbon in leach (CIL) plant, which started to operate at the end of 2012. From 2005 to the end of 2016, the accumulated production reached about 28.6 tons of gold, of which 18.7 tons by Beadell.

Unigeo observed indications of the mineralization in 1978-79, in the course of a regional campaign of geologic reconnaissance and geochemical soil sampling covering the area between the Amapari and the Araguari Rivers. During a follow-up of soil anomalies, gold in soil was found near an outcrop of iron formation, upstream on a creek where *garimpeiros* were recovering gold. Returning to the area in 1994, Unigeo found that *garimpeiros* had identified primary mineralization in the iron formation at Urucum, and, observing the favorable pattern of the mineralization, step by step covered the western ridge of the iron formation with soil sampling at intervals of 20 meters, in lines spaced of

100 meters, together with geologic mapping and sampling of outcrops and excavations opened by the *garimpeiros*. The work revealed the 8 kilometers long mineralization from Urucum to Tap AB1. Immediately after, two drilling campaigns were initiated, with reverse circulation holes for soil and saprolite, and with diamond core holes for fresh mineralization at depth. Subsequent exploration by AngloGold Ashanti, Min. Pedra Branca and Beadell lead to the identification of several gold deposits in the heavily faulted area at southeast of TapAB1 and along the southern limb of the syncline southeast of this area. More orebodies continue to be found in these areas.

The deposition of gold in the iron formation occurred when sulfur-rich auriferous hydrothermal solutions, ascending through favorable pathways in the shear zone and fault structures, reached the iron-rich minerals and reacted with them, collected iron from the magnetite and iron silicates and dumped iron and sulfur as sulfides, in the process also precipitating silica, carbonates and the gold.

The pattern and intensity of mineralization varies from place to place, from disseminations to massive ore shoots, with combined thickness of up to 25 meters (Fig. 12).

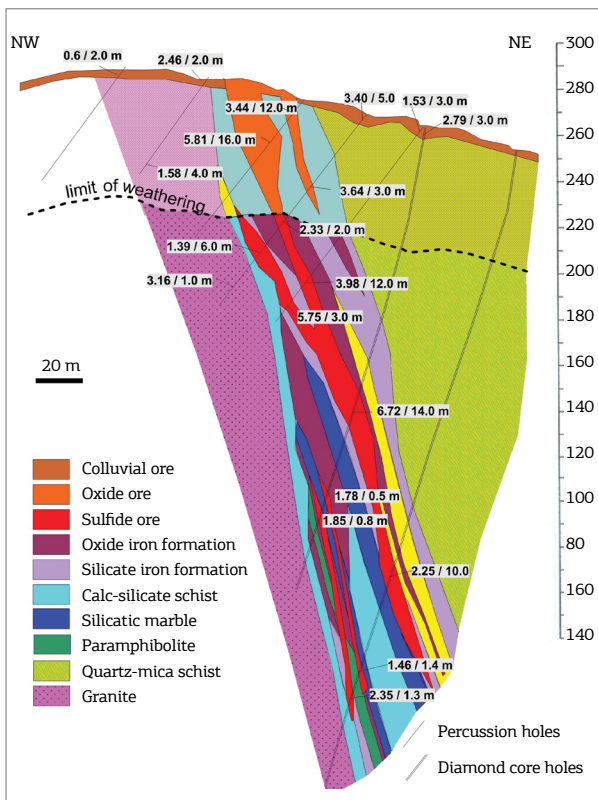


Figure 12. Initial geologic profile of the Urucum orebody, as prepared by Minorco. Mineralization is preferentially hosted in the faulted iron formation. Values next to the trace of the holes indicates grades of gold (g/t Au) and meters of mineralization.

The orebodies are composed of concentrations, bands, veins, veinlets and disseminations of fine-grained silica, carbonates and sulfides, which fill open spaces and totally or partially replace the host rocks. The initial data indicated a dominance of pyrrhotite at north and pyrite at south, followed by variable quantities of arsenopyrite, chalcopyrite and galena. Gold occurs in free form or included in the sulfides (Horikava 2008). The width of the hydrothermal alteration of the host rocks is quite narrow, limited to the very margins of the ore masses, constituted by silicification accompanied by dissemination of sulfides.

The weathering is intense, and in the mineralized zone it reaches more than 100 meters of depth. After the leaching of the soluble components of the rocks, gold was concentrated together with secondary oxides and hydroxides of iron and aluminum, residual silica and clays, forming both a rich saprolite and a rich colluvium that reaches up to 25 meters of thickness and spreads laterally downslope of the hill. Both the rich saprolite and the mineralized colluvium constitute the oxide ore and are being mined open cast, together with masses of fresh mineralization available at the bottom of the pits (Fig. 13).

When the property was sold to Wheaton Mining, the total resources estimated with the data collected by Unigeo/Minorco, reached 20 million tons at 1.8 g/t of oxide ores for surface mining, plus 8 million tons at 5.6 g/t of sulfide ores for underground mining. When Beadell took over, a new estimation of the resources indicated 23 million tons at 1.45 g/t for surface mining, plus 20 million tons at 2.21 g/t of sulfide ore. The numbers for oxide ores and surface mining are similar in both estimates, but the grade for underground operation indicates strong dilution in the Beadell's estimate (Beadell Resources 2017).

As declared by Beadell (Beadell Resources 2017), at the end of 2017 the estimated available reserves reached 20.9 million tons at 1.69 g/t Au of weathered and primary mineralization for surface mining, and 3.0 million tons at 3.61 g/t Au for underground mining at Urucum, where the first pre-feasibility study for underground mining had just finished (Fig. 14). The estimated total *in situ* resource reached 54.7 million tons at 1.97 g/t, plus 5.8 million tons at 0.63 g/t of stockpiles. These numbers are due to grow, as the company is continuously identifying new orebodies, and the known orebodies are open in depth.

At this point, it might be important to note that Beadell retains the rights to explore and exploit gold mineralization in the area of Jindal, what it is the case of the Duck Head, Woodpecker and Gold Nose gold deposits.

In a presentation to their shareholders early in 2016, Beadell Resources informed the discovery of gold mineralization in



Figure 13. North-south line of pits opened by Beadell, with Tap AB1 in the first plane, Tap AB2 and Tap C in sequence, with Urucum in the horizon, near to the high plateau of the Serra da Canga. Photo from Beadell open presentation of November of 2016.

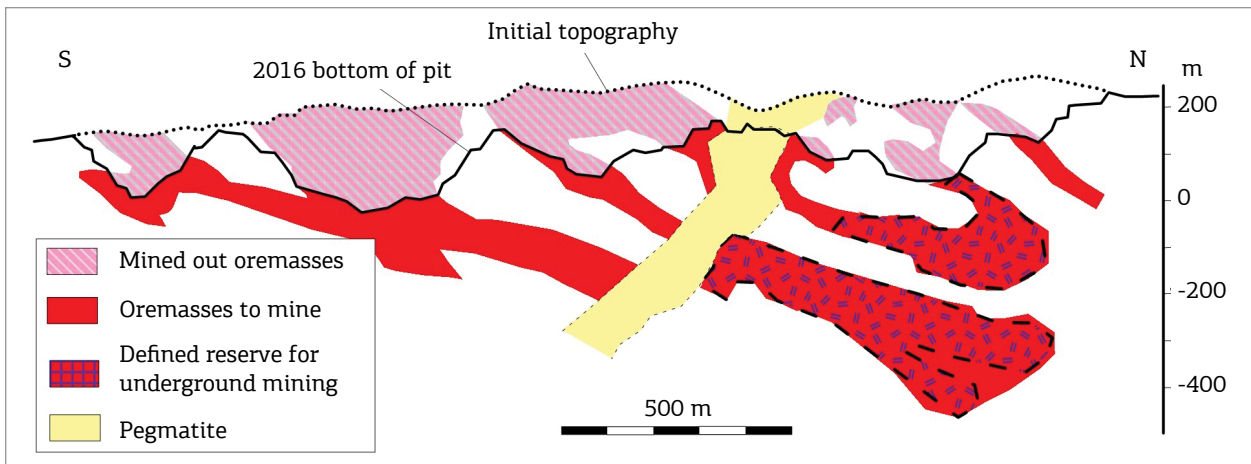


Figure 14. Longitudinal section of the 2.2 kilometers long Urucum pit, outlining exploited and unexploited portions of the main orebodies of the deposit, which plunge north, are crossed by one large pegmatite, and are open in depth. The pit surpasses 250 meters of maximum depth. At north, Beadell identified a reserve for underground mining totalling 3.0 million tons at 3.61 g/t Au. (Based on illustrations presented by Beadell Resource 2010-2017).

iron formation at Mutum, at the headwaters of the Carneiro creek, 20 kilometers east of Tucano. Initial shallow auger holes revealed values up to 5.13 g/t over 7 meters. Their initial geologic map indicates the presence of three parallel lines of iron formation oriented to north-west, with the southern of them dragged to a north-south strike for 2 kilometers, possibly following a fault. There are gold anomalies in soil over the three lines of iron formation, with the better grades coinciding to where the southern line is oriented north-south.

IRON ORE DEPOSITS, THE MINE OF JINDAL

The iron resource in the area of Jindal Group easily reaches 500 million tons of mineable iron ore. MMX Mineração explored that portion of the iron formation and, supported on a proven resource of 267 million tons, reshuffled the railway from Serra do Navio to Santana and the port formerly used by ICOMI, built one washing and concentration plant and ancillary

installations, and initiated the mining. With the operation going at full speed, it was sold to Anglo American do Brasil, included in the same deal that involved the selling of the Minas-Rio Project, in the state of Minas Gerais. During 2012, Anglo produced and sold 6 million tons. In 2013, at about the occasion when an accident affected the structure of the port, the project was sold to Zamin, which have not provided the recovery of the port and interrupted the activities. The Jindal Group has acquired the property and is recovering the mine, the port and the railway.

The accident at the port was due to the clayous and fragile nature of the margin of the Amazon River. In the engineering of the port, ICOMI avoided heavy installations at the margin of the river, installing instead a floating deck, tied to two +100 meters long vertical piles fixed in compact layers of sediment found below the fragile sediments. For nearly 50 years, the manganese ores were transported to the ships via an elevated conveyor supported on the floating deck and on a safe point away of the margin of the river. Probably ignoring the reason of that engineering and without access to the construction project, the new port operators set auxiliary installations and activities close to the the margin of the river, causing the accident.

The mineable ore varies from massive, when originated from oxidized magnetite-rich iron formation, to friable, derived from less oxidized hematite-rich iron formation (Fig. 15). In every case, magnetite is replaced by martite, silicates are leached, and limonite cements the fragments (Fig. 16). The weathering gets to more than 100 meters of depth, and invariably the outcrops are massive and very hard, formed by well cemented martite, hematite and limonite. Friable hematitic iron formation, occasionally indicated by a few residual blocks in canga, are only exposed on excavations and road cuts.

Grades, mineralogy, consistency and size of ore products vary with depth. Compact ores, good to produce lumps and natural pellets of high grade, are formed by martite-rich layers and also by rich canga formed by bulky cementation by limonite of blocks of oxidized iron formation. Friable ores, mostly made of hematitic ore, are good to produce medium- to fine-grained concentrates of good grade.

CONCLUSIONS

For question of space, the authors did not present information regarding mineral deposits and occurrences indicated in Fig. 2, but outside the limits of Fig. 3.

In general terms, the occurrences of manganese carbonates, oxides and gondites occur at the base of the column

of metasediments of the Vila Nova Group. Units of banded iron formation appear higher in the stratigraphy, form topographic ridges and are conspicuous in aerial magnetometry.

Gold occurs in a variety of environments, with the larger concentrations related to shears and faults oriented to north, a favorable direction to have open spaces for the flux of hydrothermal solutions. Iron formations and carbonatic metasediments of the Vila Nova Group are the favorite host for hydrothermal mineralizations. In this sense, it seems wise to examine geochemical anomalies of copper, zinc and lead in the areas where hydrothermalism is identified.

Mafic-ultramafic layered complexes intrude the Vila Nova Group and have potential for chromite and magnetite, as seen at Santa Maria with the Bacuri deposit, besides eventual platinum group elements, nickel and vanadium. These complexes rarely outcrop, their presence suggested

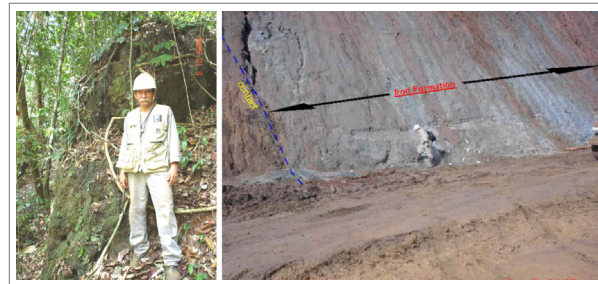


Figure 15. Exposures of iron formation in the area of Jindal. Left, outcrop of the ore, represented by a massive and erosion resistant magnetite/martite-rich unit. Right, exposed on a road cut, the friable hematitic iron formation, a type that never outcrops and is the favorite for mining due to its high grade and low cost to mine and process.



Figure 16. Above, fresh iron formation constituted by bands of magnetite, quartz and silicates. Below, weathered, with layers of martite and hematite replacing magnetite, and with limonite replacing silicates and most of the quartz. The texture of the bands varies from massive to friable. Open spaces indicate where minerals were completely leached out.

by magnetometry, soil geochemistry, and a thick cover of canga poor in quartz and other resistant primary minerals.

Alluvial concentrations of cassiterite and tantalite-columbite derive from pegmatites related to the syntectonic granites that intrudes the Vila Nova Group. A dedicated exploration campaign for large tantalum-bearing pegmatites would be acceptable.

ACKNOWLEDGEMENTS

The authors thank Prof. Dr. Umberto G. Cordani for the invitation to prepare this note and for the time, dedication and patience devoted to have it brought to the patterns and style adopted by the journal.

REFERENCES

- Beadell Resources. 2017. Informations regarding Tucano and Mutum. Available at: <http://www.beadellresources.com.au> [cited at Jul. 2017].
- Chisonga B., Gutzmer J., Beukes N.J., Huizenga J.M. 2012. Nature and origin of the protolith succession to the Paleoproterozoic Serra do Navio manganese deposit, Amapá Province, Brazil. *Ore Geology Reviews*, **47**:59-76.
- Cordani U.G., Ramos V., Fraga L.M., Cegarra M., Delgado I., Souza K.G., Gomes F.E.M., Schobbenhaus C. 2016. *Tectonic Map of South America, second edition, 1:5,000,000*. Commission for the Geologic Map of the World.
- Cordani U.G. & Teixeira W. 2007. Proterozoic accretionary belts in the Amazonian Craton. *Geological Society of America Memoir*, **200**:297-320.
- Dorr J.V.N., Park Jr. C.F., Paiva G. 1950. Manganese deposits of the Serra do Navio District, Territory of Amapá, Brazil. *United States Geological Survey Bulletin*, **964**(A):1-39.
- Dorr II J.V.N., Park Jr. C.F., Paiva G. 1950. *Depósito de Manganês do Distrito de Serra do Navio, Território Federal do Amapá*. DNPM-DFPM, bol. 85
- Horikava E.H. & Ferreira Filho C.F. 2003. Corpos Máficos-Ultramáficos Acamadados da Região da Serra do Navio. In: VIII Simpósio de Geologia da Amazônia, Expanded Abstracts, Sociedade Brasileira de Geologia, CD-ROM.
- Horikava E.H. 2008. *Geoquímica de Solo e Geologia da Região do Depósito de Ouro do Amapari – AP*. MS Dissertation, Universidade Federal de Minas Gerais, 2 vol.
- Kroonenberg S.B., Roeber E.W.F., Fraga L.M., Reis N.J., Faraco M.T., Lafon J.M., Cordani U., Wong T.E. 2016. Paleoproterozoic evolution of the Guiana Shield in Suriname: A revised model. *Netherlands Journal of Geosciences*, **95**(4):491-522.
- Lafon J.M., Tavares R.P.S., Tassinari C.C.G., Barros C.E.M. 2008. Idade, Caracterização Geoquímica e Isótopos de Nd dos Anfíbolitos do Grupo Vila Nova e Granitóides Associados na Serra do Navio, Borda Norte do Bloco Arqueano Amapá: Implicações Geodinâmicas. In: Anais Congresso Brasileiro de Geologia, 44, Curitiba, p. 59.
- Leinz V. 1948. Estudo Genético do Minério de Manganês da Serra do Navio, Território do Amapá. In: Anais da Academia Brasileira de Ciências, Ano XX, **2**:213-221.
- Lima M, Montalvão R, Issler R, Oliveira A, Basei M., Araujo J., Galeão da Silva G. 1976. *Folha NA/NB.22, Macapá*. Projeto Radam; MME-DNPM Levantamento de Recursos Naturais, V-6, Geologia,
- Marotta C.A., Scarpelli W., Maruo J., Barbour A.P., Lima L.G.B. 1966. *Notas sobre o Distrito Manganífero de Serra do Navio*. Anais da VI Conf.Geol. Guiana, DNPM, Avulso 41, 57-69
- Marzoli A, Renne P.R., Piccirillo E.M., Ernesto M., Bellieni G., De Min A. 1999. Extensive 200-million-year-old continental flood basalts of the Central Atlantic Magmatic Province. *Science*, **284**(5414):616-618.
- Nagell R.H. & Silva A.R. 1960. O Carbonato de Manganês como Protominério no Distrito de Serra do Navio. In: XIV Congresso da Sociedade Brasileira de Geologia, Brasília.
- Nagell R.H. 1962. Geology of the Serra do Navio manganese district, Brazil. *Economic Geology*, **57**(4):482-498.
- Rodrigues O.B., Kosuki R., Coelho Filho A. 1986. *Distrito Manganífero de Serra do Navio, Amapá*. Principais Depósitos Minerais do Brasil. In: Ferro e Metais da Indústria do Aço. Departamento Nacional da Produção Mineral, Vol II, Cap XIV.
- Rosa-Costa L.T., Lafon J.M., Delor C. 2006. Zircon geochronology and Sm-Nd isotopic study: Further constraints for the Archean and Paleoproterozoic geodynamical evolution of the southeastern Guiana Shield, north of the Amazonian Craton, Brazil. *Gondwana Research*, **10**(3-4):277-300.
- Scarpelli W. 1966. Aspectos genéticos e metamórficos das rochas do Distrito de Serra do Navio. In: Anais da VI Conferência Geológica das Guianas, DGM-DNPM, Avulso 41, p. 37-56.
- Scarpelli W. 1968. *Precambrian Metamorphic Rocks of Serra do Navio, Brazil*. Unpublished Report on Student Research Project, Stanford University.
- Scarpelli W. 1973. *The Serra do Navio Manganese Deposit (Brazil)*. In: Unesco – Proceedings of the Kiev Symposium on the Genesis of Precambrian Iron and Manganese Deposits, p. 217-228.
- Schobbenhaus C., Campos D.A., Derze G.R., Asmus H.E. 2001; *Mapa Geológico do Brasil e da Área Oceânica Adjacente incluindo Depósitos Minerais; 1:2,500,000*; DGM-DNPM
- Silva A.R, Scarpelli W., Marotta C.A. 1963. Contribuição ao Estudo dos Protominérios de Manganês do Distrito de Serra do Navio. *Boletim da Sociedade Brasileira de Geologia*, **12**:37-48.
- Spier C.A. & Ferreira Filho C.F. 2001. The chromite deposits of the Bacuri Mafic-Ultramafic Layered Complex, Guyana Shield, Amapá State, Brazil. *Economic Geology*, **96**(4):817-835.
- Tavares R.P.S. 2009. *Granitóides e Anfíbolitos da Serra do Navio, Borda Norte do Bloco Arqueano Amapá: Caracterização Petrográfica e Geoquímica, Geocronologia Pb-Pb em Zircão e isótopos de Nd*. MS Dissertation, Universidade Federal do Pará.
- Valarelli J.V. 1967. *O Minério de Manganês da Serra do Navio, Amapá*. PhD Thesis, Universidade de São Paulo, São Paulo.

Available at www.sbgeo.org.br